behavior of the dosimetry system. This lecture will describe some of the most employed multichannel methods: its assumptions, formulas, uncertainties, and weaknesses. Multichannel film dosimetry can deliver more accurate doses, mainly by mitigating spatial heterogeneities in the film-scanner response, in particular, variations in the active layer thickness. This lecture will also explain which sources of uncertainty are reduced by using multichannel methods and what other corrections can we apply to improve radiochromic film dosimetry.

**SP-0666 Developments in time-resolved detectors**

A. Rozenfeld[1]
*[1]Centre for Medical Radiation Physics, University of Wollongong, University of Wollongong, Australia*

**Abstract text**
A range of silicon-based dosimeters has been made available to address the challenges of ensuring an ever safer and more accurate treatment delivery in radiotherapy. These dosimeters, extensively used in the clinic, possess a set of convenient features: a response which is stable and linear with deposited dose, and the possibility of manufacturing sensitive volumes sufficiently small while retaining relatively high sensitivity. The present lecture reviews, in terms of design, applications and limitations, innovative silicon dosimeters able of high-spatial and temporal resolution which are being developed at the Centre for Medical Radiation Physics (CMRP).

Monolithic diode arrays with spatial resolution better than 2mm and temporal resolution better than 0,1ms are discussed for dose QA in a heterogeneous fully customized phantom for IMRT and VMAT treatments with small photon fields that dynamically track the tumor motion using dynamic multi-leaf collimator (DMLC). Diode arrays with spatial resolution as high as 0.05 mm for in body application for *in vivo* real time source dwelling position and time verification in high dose rate (HDR) and immediate source position as dropped in low dose rate (LDR) brachytherapy with submillimetre spatial resolution are discussed. Finally, the use of a MOS*kin*, a metal-oxide-semiconductor field-effect
transistor (MOSFET) and innovative epi-diode detectors for time resolved rectal wall dosimetry and source tracking in gynaecological multi catheter applicator respectively in HDR brachytherapy are presented

**Proffered Papers: PH 14: Proffered paper: Treatment planning of proton therapy**

**OC-0667 Experimental assessment of inter-centre variation and accuracy in SPR prediction within the EPTN**

N. Peters[1,2], P. Wohlfahrt[1], A. Bolsi[3], C.V. Dahlgren[4], L. De Marzi[5], M. Ellerbrock[6], F. Fracchiolla[7], J. Free[8], C. Gomà[9], J. Góra[10], T. Kajdrowicz[11], R. MacKay[12], S. Molinelli[13], O. Nørrevang[14], I. Rinaldi[15], V. Rompokos[16], P. Van der Tol[17], X. Vermeren[18], C. Richter[1,2,19,20]
*[1]OncoRay – National Center for Radiation Research in Oncology, Faculty of Medicine and University Hospital Carl Gustav Carus- Technische Universität Dresden-Helmholtz-Zentrum Dresden - Rossendorf, Dresden, Germany ; [2]Helmholtz-Zentrum Dresden-Rossendorf, Institute of Radiooncology - Oncoray, Dresden, Germany ; [3]Paul Scherrer Institut, Center for Proton Therapy, Villigen, Switzerland; [4]The Skandion Clinic, Skandionkliniken, Uppsala, Sweden; [5]Institut Curie, Centre de protonthérapie, Orsay, France; [6]Heidelberg Ion-Beam Therapy Center HIT, Department of Radiation Oncology- Heidelberg University Hospital, Heidleberg, Germany ; [7]APSS Trento, Centro di Protonterapia di Trento, Trento, Italy; [8]University of Groningen-University Medical Center Groningen, Department of Radiation Oncology, Groningen, The Netherlands ; [9]KU Leuven, Department of Oncology, Leuven, Belgium ; [10]EBG MedAustron GmbH, Medizinische Strahlenphysik, Wiener Neustadt, Austria ; [11]Institute of Nuclear Physics, Polish Academy of Sciences, Krakow, Poland ; [12]University of Manchester, Faculty of Life Sciences, Manchester, United Kingdom ; [13]Centro Nazionale di Adroterapia Oncologica, Department of Medical Physics, Pavia, Italy; [14]Danish Centre for Particle Therapy, Aarhus University, Aarhus, Denmark ; [15]Maastro Clinic, Maastricht, The Netherlands; [16]University College London Hospitals, Department of Radiotherapy, London, United Kingdom ; [17]HollandPTC, Protonen Therapie Centrum, Delft, The Netherlands; [18]Universitätsklinikum Essen, Westdeutsches Protonentherapiezentrum Essen, Essen, Germany ; [19]Faculty of Medicine and University Hospital Carl Gustav Carus- Technische Universität Dresden, Department of Radiotherapy and Radiation Oncology, Dresden, Germany ; [20]German Cancer Consortium DKTK-partner site Dresden, German Cancer Research Center DKFZ- Heidelberg, Dresden, Germany*

**Purpose or Objective**
The standard approach for CT-number to stopping-power-ratio (SPR) conversion in particle therapy is the use of a heuristic stepwise translation, a so-called Hounsfield look-up table (HLUT). It is defined by each treatment facility individually and depends on both the calibration method and CT scan protocol. A recent survey has shown broad variability in these parameters [1], making a simple comparison on HLUT level unfeasible. Hence, we present a comprehensive experimental evaluation of inter-centre variation and absolute accuracy in SPR prediction within the European Particle Therapy Network (EPTN).

**Material and Methods**
A head and a body phantom with 17 tissue surrogate inserts were scanned consecutively at the participating centres using their individual clinical scan protocol. The inserts were tissue-equivalent concerning particles; their composition and SPR were blinded for the participants. The SPR calculation was performed using each centre's CT scan and HLUT (Fig.1).The inter-centre variation and absolute accuracy in SPR prediction were quantified for each tissue surrogate individually and then summarised into the relevant tissue groups: lung, soft tissues and bones. Finally, to evaluate the integral effect on range prediction for typical clinical beams traversing different tissues, for three simplified beam paths the determined SPR deviations were accumulated according to their respective tissue distribution. So far, data from 9 out of 17 participating centres was available.

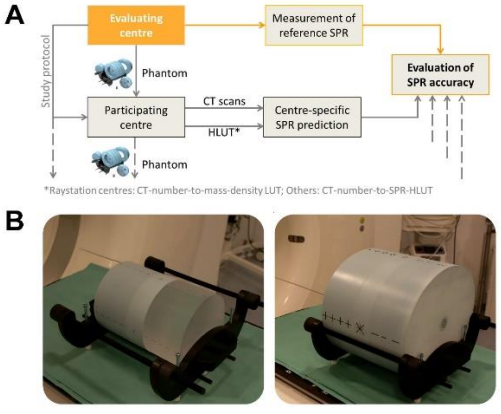


***Figure 1: (A)*** *Scheme of the study design. SPR: Stopping power ratio; HLUT: Hounsfield look-up table.* ***(B)*** *Experimental setup of the head (left) and body phantom (right) with the tissue surrogates inserts placed in the centre part of each phantom.*

**Results**

A 2σ inter-centre variation in SPR prediction of 5.7% and 5.5% relative to water was determined for the bone inserts in the head and body setup, respectively. Comparable results were achieved for the lung tissue surrogates (6.4% and 2.2%). In the soft tissue region an overall higher accuracy was achieved with a variation below 0.9% in both setups and a mean SPR prediction accuracy below 0.5%. In the head setup, both lung tissues and bones were overestimated in most centres, while in the body setup the bones were underestimated (Fig. 2A). For the three exemplary beam paths, inter-centre variations in relative range were 1.5% on average. In specific centres, range deviations from reference exceeded 1.5% (Fig 2B).

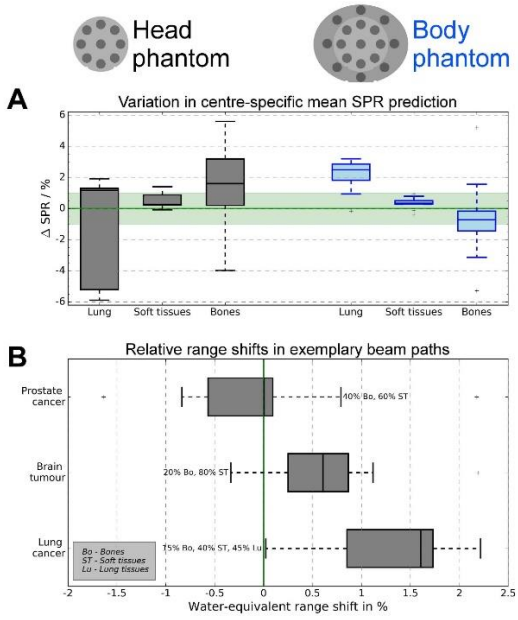


***Figure 2: (A)*** *Variations in stopping-power-ratio (SPR) prediction between 9 centres. The 17 tissue surrogates were classified into the relevant tissue groups lung (2), soft tissues (11) and bones (4) and then averaged centrewise.* ***(B)*** *Resulting range shifts relative to water along three simplified beam path scenarios, resulting from an accumulation of the SPR deviations in the three tissue groups weighted with their relative contribution in the beam path. Whiskers in boxplot are defined by last values within 1.5x interquartile range.*

**Conclusion**

Large inter-centre variations in SPR prediction were observed in low- and high density tissue surrogates. The differences in deviation for bone between the two setups indicate a strong influence of scanning parameters such as the level of beam hardening correction, potentially resulting in range shifts of clinical relevance. As the study allows for a direct attribution of the measured deviations to the calibration methods and scan protocols used by the individual centres, it stresses the need for inter-centre standardisation. While this work addresses the accuracy in SPR prediction under idealised study conditions, a direct conclusion on overall range accuracy in patients is not possible. The study is currently still ongoing.

*[1] Taasti et al. 2018, phiRO 6 25-30*

## OC-0668 MRI-only proton therapy treatment planning with synthetic CT images generated using deep learning

A.M. Barragán Montero[1,2], K. Souris[1], S. Kazemifar[2], R. Timmerman[3], S. Jiang[2], X. Geets[1], E. Sterpin[1], A. Owrangi[2]

*[1]Université Catholique de Louvain- Institute of Experimental & Clinical Research, Molecular Imaging-Radiotherapy and Oncology MIRO, Brussels, Belgium ; [2]UT Southwestern Medical Center, Medical Artificial Intelligence and Automation MAIA, Dallas, USA ; [3]UT Southwestern Medical Center, Radiation Oncology, Dallas, USA*

**Purpose or Objective**

To evaluate the dosimetric accuracy of proton therapy treatment planning using synthetic CT images generated from magnetic resonance images (MRI) with a generative adversarial network (GAN).

**Material and Methods**

The GAN is a type of unsupervised deep learning algorithm that uses two neural networks that compete against each other: one network generates synthetic CT (sCT) candidates (generator), while the other evaluates them by comparison with real CT images (discriminator). This process is repeated until the discriminator cannot distinguish anymore between the real and synthetic CT, which entails that the generator learnt to accurately transform MR to CT images. The model was trained with (T1-weighted) MRI and CT slices from 63 brain cancer patients, and tested separately in 12 different patients. Synthetic CT images of the same patients were rigidly registered to the CT images using mutual information. Proton pencil beam scanning plans were created on the real CT of the 12 test patients, using RayStation v5.99 (RaySearch Laboratories AB), and recomputed on the sCT for dosimetric comparison. Robust optimization on the CTV with 3% range uncertainty and 3mm accounting for setup error was used to create the plans.

**Results**

The average absolute error between the dose computed on the CT and sCT for the 12 test patients, and its standard deviation (SD), on the mean (Dmean) and maximum dose (Dmax) for relevant organs in the nominal case is presented in Table 1. For the CTV, the error on the dose delivered at 95% (D95) and 5% (D5) of the volume is also reported. Overall, the error remained below 2.5% of the dose prescription (60 Gy in all patients), for all considered metrics. Figure 1.a shows the DVH for one of the test patients, with overlapping lines for the dose on the CT (solid line) and sCT (dotted line). Figure 1.b and 1.c show the dose distribution on the same patient for CT and sCT, respectively, for a slice on the center of the target volume. The generation of a full 3D sCT for a given set of MRI slices took only 9 s.

| | | Average (%) | SD |
|---|---|---|---|
| CTV | D95 | 0,43 | 0,41 |
| | D5 | 0,52 | 0,40 |
| | $D_{mean}$ | 0,28 | 0,21 |
| Brainstem | $D_{max}$ | 1,29 | 1,69 |
| | $D_{mean}$ | 0,40 | 0,43 |
| Optic chiasm | $D_{max}$ | 0,86 | 0,63 |
| | $D_{mean}$ | 1,36 | 1,10 |
| Optic Nerve L | $D_{max}$ | 2,43 | 2,34 |
| | $D_{mean}$ | 1,38 | 1,29 |
| Optic Nerve R | $D_{max}$ | 1,81 | 2,38 |
| | $D_{mean}$ | 0,46 | 0,66 |

**Table 1.** Average absolute error between the dose on CT and sCT for the test patients, and its standard deviation (SD), expressed as % of the dose prescription.